

DOI: 10.1002/ejoc.201901772



Wavelength Tuning | Very Important Paper |

Linker-Free Near-IR Aza-BODIPY-Glutamine Conjugates Through Boron Functionalization

Maodie Wang,^{[a][‡]} Guanyu Zhang,^{[a][‡]} Nichole E. M. Kaufman,^[a] Petia Bobadova-Parvanova,^[b] Frank R. Fronczek,^[a] Kevin M. Smith,^[a] and M. Graca H. Vicente*^[a]

Abstract: A series of linker-free aza-BODIPY-glutamine conjugates were synthesized and investigated, both experimentally and computationally. The structures of the aza-BODIPYs were confirmed spectroscopically, and in the case of **3a** an X-ray structure was obtained. All aza-BODIPYs show intense absorption bands between 642–667 nm and fluorescence emissions between 691–703 nm. The fluorescence quantum yields of the 2,6-unsubstituted compounds **1a–4a** were found to be $\Phi_f \approx 0.2$ in chloroform, while those of the corresponding 2,6-dibromi-

nated derivatives **1b–4b** were less than 0.01. The cytotoxicity and cellular uptake of all aza-BODIPYs were investigated in human carcinoma HEp2 cells. The most cytotoxic aza-BODIPYs were found to be **3a** and **3b**, due to the presence of the cyclic *N,O*-bidentate amino acid ring, rather than the presence of the 2,6-bromine atoms. The results show that the mode of glutamine conjugation to the aza-BODIPY determines the stability and cytotoxicity of the conjugates.

Introduction

Photodynamic therapy (PDT) is a minimally-invasive technique for the treatment of various cancers and infections. PDT involves the activation of a photosensitizer (PS) by light in the presence of oxygen, which generates singlet oxygen ($^{1}O_{2}$) and other reactive oxygen species (ROS), that destroy tumor cells via necrosis, apoptosis and/or autophagy-associated cell death. Effective photosensitizers generally display high quantum yields of photosensitizer triplet state ($\Phi_{T} > 0.4$), triplet state lifetimes ($\tau_{T} \approx 1~\mu s$) and triplet energy ($E_{T} \geq 95~kJ~mol^{-1}$), for efficient energy transfer to triplet molecular oxygen, along with high molar extinction coefficients and low dark cytotoxicity.

The first aza-dipyrromethene was reported by Rogers in 1943 and investigated as a coloring agent. [2] Subsequently, several aza-dipyrromethene derivatives were synthesized and their properties and potential applications were investigated. Among these, the BF₂-azadipyrromethenes, designated aza-BODIPYs, have attracted much research due to their excellent spectroscopic properties. [3] Aza-BODIPYs characteristically display sharp absorption and emission bands in the visible and near-IR region of the optical spectrum, with high molar extinction coefficients, and good solubility and stability in both organic and aqueous media. Furthermore, aza-BODIPYs that absorb light in the thera-

peutic window (650–800 nm) can be synthesized, where there is reduced tissue autofluorescence and scattering, and increased tissue penetration. To date, aza-BODIPYs have been widely applied in optoelectronics and solar energy materials, photoredox catalysts, as photosensitizers for PDT, and as near-IR optical sensors.^[3,4]

It has been previously shown that the introduction of heavy halogen atoms at the 2- and 6-positions of aza-BODIPYs, enhances intersystem crossing and the triplet state quantum yield. O'Shea and co-workers studied several PDT photosensitizers based on aza-BODIPY structures. To enhance biocompatibility and photodynamic activity, aza-BODIPY dyes are normally modified on their phenyl rings to achieve enhanced water solubility and selectivity for tumor cell targeting. On the other hand, boron functionalization has emerged as a powerful tool to increase the fluorescence quantum yield, Stokes shift, solubility and stability of BODIPYs and aza-BODIPYs. This approach also reduces the self-aggregation of aza-BODIPYs and was used to obtain water-soluble aza-BODIPY-anti-PD-L1 bioconjugates for tumor imaging.

Recently, we developed a convenient one-pot reaction methodology for introducing amino acids onto the boron atom of BODIPYs to produce linker-free BODIPY-glycine conjugates. [7d] L-Glutamine, the most abundant naturally occurring amino acid in humans, plays a significant role as a nitrogen shuttle for circulating ammonia in the human body. [9] Furthermore, glutamine is crucial for protein and glutathione synthesis, energy production, and beneficial for minimizing infection in trauma and surgery patients. Herein, we report the synthesis of linker-free near-IR aza-BODIPY-glutamine conjugates, bearing one or two amino acids, and their spectroscopic and in vitro investigations.

 [[]a] Department of Chemistry, Louisiana State University Baton Rouge, LA 70803, USA E-mail: Vicente@Isu.edu

[[]b] Department of Chemistry, Rockhurst University Kansas City, MO 64110, USA E-mail: petia.bobadova@rockhurst.edu

 $^{[\}pm]$ M. W. and G. Z. contributed equally.

Supporting information and ORCID(s) from the author(s) for this article are available on the WWW under https://doi.org/10.1002/ejoc.201901772.





Results and Discussion

Synthesis

Following our previously reported synthetic procedure. [7d] aza-BODIPYs 2a-4a were synthesized from in situ generated BCl₂/ aza-BODIPY by reaction of 1a with boron trichloride, followed by addition of 5 equivalents of $N\alpha$ -(tert-butoxycarbonyl)-L-glutamine under basic conditions, as shown in Scheme 1. N-Boc protected L-glutamine was used to avoid the formation of additional by-products obtained when unprotected L-glutamine was employed, therefore increasing product yields, and to facilitate the purification and characterization of the products. Furthermore, in the case of the cyclic N,O-bidentate BODIPYs,[7d] an electron-withdrawing group on the nitrogen atom is necessary for decreasing the charge on boron, leading to stable N(sp³)-BODIPYs. This two-step one-pot reaction gave 25.7 % of the mono-substituted product 2a and 10.5 % of the cyclic N,O-bidentate product 3a, along with 7.8 % of the di-substituted product 4a. This unusual product distribution is probably caused by the steric hindrance of the 3,5-phenyl rings. Indeed, computational modeling (see below) shows that the cyclic product 3a is 18.3 kcal/mol less stable than 2a and that the diproduct 4a is 26.3 kcal/mol less stable than 2a. The bromination of 1a-4a was carried out in chloroform using 2.2 equivalents of N-bromosuccinimide (NBS) giving the corresponding 2,6-dibrominated products 1b-4b in quantitative yields. Among the three brominated products, again, the mono-substituted 2b is the most stable, with the cyclic N,O-bidentate 3b being 28.4 kcal/mol and the di-substituted 4b being 44.4 kcal/mol higher in energy compared with 2b. The structures of aza-BODI-PYs were confirmed by high resolution mass spectrometry, and by ¹H, ¹¹B and ¹³C NMR spectroscopy (see Supplementary Materials, Figures S1-S18). All compounds were stable in aqueous solutions under neutral conditions for several days, as previously reported for BODIPY-glycine conjugates substituted at the boron atom.[7d]

Crystallography

Suitable crystals of aza-BODIPY **3a** for X-ray analysis were obtained by slow evaporation of dichloromethane and hexane. The result is shown in Figure 1. In the crystal of **3a**, the four independent aza-BODIPY molecules differ somewhat in the conformations of their substituents, but their aza-BODIPY cores are very similar. They exhibit mean 12-atom deviation from coplanarity of 0.076 Å over the four molecules, and the core ring system has a slightly bowed conformation, with the carbon atoms at the 2 and 6 positions lying an average of 0.147 Å out of the plane. The 1,7-phenyl rings form dihedral angles with the aza-BODIPY core in the range 13.8–25.9°, with mean (of 8) 19.9°. The 3,5-phenyl rings are somewhat more nearly orthogonal to the core, forming dihedral angles in the range 54.3–74.6°, with mean (of 8) 66.6°.

Photophysical Properties

The spectroscopic properties of aza-BODIPYs **1a-4a** and their dibrominated derivatives **1b-4b** were investigated in chloro-

Scheme 1. Syntheses of aza-BODIPY-Gln conjugates 2a-4a and 2b-4b.

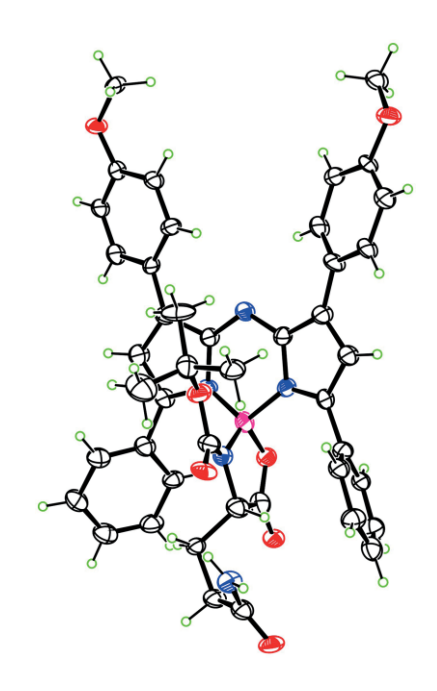


Figure 1. Crystal structure of aza-BODIPY 3a with 50 % ellipsoids.

form, and the results are summarized in Table 1 and shown in Figure 2. The maximum absorption and emission wavelengths, molar extension coefficients, fluorescence quantum yields, and Stokes shifts were determined. All compounds show a strong S_0 to S_1 transition with the maximum absorbance wavelength between 642 and 667 nm, depending on the substituents at the boron core. The molar extinction coefficients of aza-BODl-PYs **2a–4a** and **2b–4b** varied from 33 800 to 53 300 m⁻¹ cm⁻¹, which are similar to those of clinically approved PDT agents, such as Temoporfin (Foscan®) and Talaporfin (Laserphyrin®).^[4]

972





Table 1. Experimental and M06-2X/6-31+G(d,p) calculated spectroscopic properties of aza-BODIPYs in CHCl₃ at room temperature. The leading transition is $S_0 \rightarrow S_1$ for all compounds.

Compound	λabs [nm] Exp	λabs [nm] Calc	Band Gap [eV]	$arepsilon$ [M $^{-1}$ cm $^{-1}$]	Oscillator Strength	$\lambda_{\sf em}$ [nm]	$\Phi_{f}^{[a]}$	Stokes shift [nm]
1a	664	594	3.70	78 000	0.90	691	0.23	27
2a	664	612	3.64	53 300	0.79	697	0.32	33
3a	642	572	3.84	33 800	0.74	696	0.13	54
4a	667	593	3.72	47 300	0.74	703	0.23	36
1b	653	576	3.83	72 800	0.91	692	< 0.01	39
2b	654	580	3.82	41 100	0.79	693	< 0.01	39
3b	644	569	3.88	36 100	0.80	696	< 0.01	52
4b	648	584	3.81	53 200	0.74	699	< 0.01	51

[a] Aza-BODIPY 1a ($\Phi_f = 0.23$ in CHCl₃)^[10] were used as the standard for BODIPYs **2a-4a** and **1b-4b**.

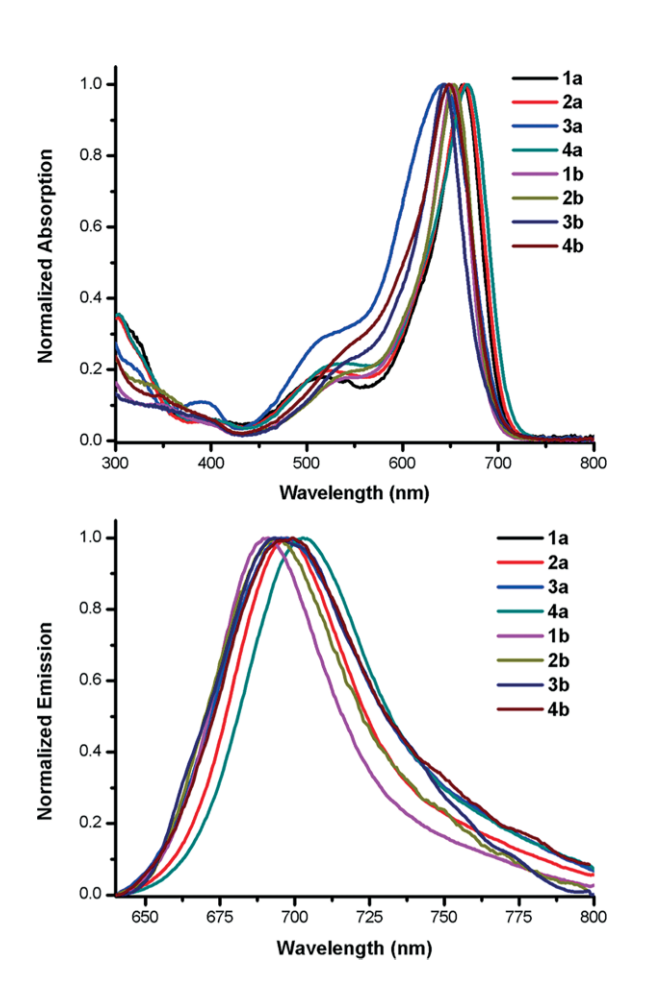


Figure 2. Absorption (top) and emission (bottom) spectra of aza-BODIPYs **1a–4a** and **1b–4b** in CHCl₃.

Interestingly, the cyclic *N*,*O*-bidentate compounds **3a** and **3b** show hypsochromic-shifted absorbance bands compared with the corresponding BF₂-aza-BODIPYs and the non-cyclic aza-BODIPY-Gln conjugates. On the other hand, the di-Gln products **4a** and **4b** show bathochromic-shifted emissions compared with all other aza-BODIPYs in this series. These values likely result from the structural features of the boron-substituted aza-BODIPYs, which may affect the dihedral angles of the 1,3,5,7-phenyl groups (see computational modeling section below).

As expected, the 2,6-dibrominated aza-BODIPYs **1b–4b** show very low fluorescence quantum yields ($\Phi_{\rm f}<0.01$) compared with the corresponding 2,6-unsubstituted products **1a–4a** (0.13 < $\Phi_{\rm f}<0.32$), due to enhanced intersystem crossing from the excited singlet to the triplet state because of spin-orbit coupling by the heavy atom effect. In addition, the 2,6-dibrominated compounds also show enhanced production of singlet oxygen, the principal cytotoxic species in PDT (see Table 2). The 2,6-dibrominated aza-BODIPY derivatives **1b**, **2b** and **4b** also show moderate hypsochromic shifts in their maximum absorbance (10–19 nm), while **3b** shows a small (2 nm) bathochromic shift.

Table 2. Comparative singlet oxygen quantum yield and in vitro dark and photocytotoxicity of aza-BODIPYs. Cells were incubated with aza-BODIPYs for 24 h prior to irradiation with 1.5 J/cm².

Compound	Dark Toxicity (IC ₅₀ , μм)	Phototoxicity (IC ₅₀ , μм)	$\Phi_{\Delta}{}^{[a]}$
1a	103 ± 4	94 ± 7	0.08
2a	120 ± 4	63 ± 5	0.12
3a	26 ± 2	20 ± 5	0.12
4a	61 ± 3	60 ± 8	0.18
1b	68 ± 5	63 ± 5	0.64
2b	45 ± 3	51 ± 4	0.54
3b	26 ± 1	24 ± 2	0.66
4b	31 ± 3	29 ± 4	0.12

[a] Methylene Blue $(\Phi \Delta = 0.52)^{[11]}$ was used as the standard for BODIPYs **1a**-**4a** and **1b**-**4b**.

Computational Modeling

Computational modeling of BODIPYs **2a–4a** and **2b–4b** reveals that these compounds are sterically congested. The boron substitution with large *N*-Boc-L-glutamine is experimentally difficult, especially in the di-substituted compounds **4a** and **4b**, and this might explain the product distribution obtained in this reaction. Interestingly, there are two conformers for compounds **1a** and **1b**, and **4a** and **4b**, respectively, depending on the orientation of the Gln carbonyl group(s). In all four cases, the *up*-conformer is more stable, which is consistent with our previous findings for BODIPY-Gly conjugates.^[7d]

The BODIPY cores for all modeled compounds (**1a-4a** and **1b-4b**) are slightly non-planar with deviation from planarity around 3–7° without noticeable trends. In all the aza-BODIPYs, the 1,7-phenyl substituents are parallel to each other and form





angles of around 24-28° for compounds 1a-4a and 28-41° for brominated 1b-4b with respect to the BODIPY core. These dihedral angles are relatively similar within the series of brominated (1b-4b) or the series of non-brominated compounds (1a-4a), with the brominated aza-BODIPYs displaying larger angles suggesting less conjugation. This is consistent with the observed bathochromic shifts for the brominated aza-BODIPYs.

On the other hand, the 3,5-phenyl substituents are not parallel, forming a larger cavity on one side of each aza-BODIPY. where the bulky Boc-protecting group of glutamine lies in the case of aza-BODIPYs 3a and 3b (see Figure S19 in the Supplemental Materials). These angles vary within the series with the brominated compounds having, in general, larger angles (56-80° for **1b–4b** vs. 36–56° for **1a–4a**). Noticeably, the cyclic compounds 3a and 3b have the largest dihedral angles within the series with **3b** approaching perpendicular. This likely happens to accommodate the large Gln-Boc substituent, and leads to the observed hypsochromic shifts.

The calculated maximum absorption wavelengths and the respective oscillator strengths are given in Table 1, while the shapes and energies of the frontier molecular orbitals of aza-BODIPYS 2a and 2b are given in Figure 3. The frontier orbitals shapes and energies of all studied aza-BODIPYs are given in the Supplemental Materials, Figure S20. The shapes of the HOMOs and the LUMOs are similar. There is a significant contribution of the 1,7-substituents, especially to the HOMOs. This is consistent with the bathochromic shifts observed for these compounds compared with their non-brominated analogs. There is almost no contribution from the boron 4,4'-substituents to the frontier orbitals. From Figure S20 the contribution of the 3,5-substituents to the electron densities of all HOMOs and LUMOs decreases when glutamine is attached, and it is minimal for aza-BODIPYs 3a and 3b. This is consistent with the largest dihedral angles found for these compounds, and consequently the least conjugation.

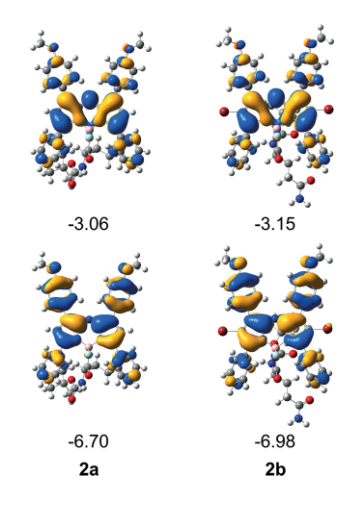


Figure 3. Frontier orbitals of aza-BODIPYs 2a and 2b. Modelled in CHCl₃. Orbital energies in eV.

Upon 2,6-dibromo substitution, the shape of the LUMO does not change significantly but the Br p-orbitals contribute to all HOMOs. The substitution stabilizes both HOMO and LUMO but the band gap remains, in general, approximately the same.

The performed calculations confirm the hypsochromic shifts observed for the cyclic compounds 3a and 3b compared with the other aza-BODIPYs from the series. This is probably due to the stabilization of HOMOs of **3a** and **3b** as seen in Figure S20. It is also consistent with the observed greater dihedral angles between the 3,5-phenyl substituents and the aza-BODIPY core, as discussed above. The calculated oscillator strengths of all aza-BODIPY-Gln derivatives are similar and lower than the corresponding BF₂-aza-BODIPY analogs. The spin-orbit interaction is not explicitly included in the present calculation. The observed fluorescence quenching for all brominated compounds is consistent with the heavy atom effect and energy transfer to the T₁ excited state.

Cellular Properties

The concentration-dependent uptake, dark and photo (light dose ≈ 1.5 J/cm²) cytotoxicities, using a Cell Titer Blue assay, of all aza-BODIPYs were investigated in human carcinoma HEp2 cells. The results are summarized in Table 2 (see also Supplementary Materials Figures S21-S23). In addition, the comparative singlet oxygen quantum yields of the BODIPYs relative to methylene blue (Φ_{Λ} = 0.52) were determined,^[11] and the results are also shown in Table 2. In general, the 2,6-dibrominated aza-BODIPYs were found to be more toxic in the dark (31 μ M < IC₅₀ < 68 μм) than the corresponding 2,6-unsubstituted derivatives (61 μ M < IC₅₀ < 120 μ M), with exception of aza-BODIPY **3b** which showed similar cytotoxicity to **3a** (IC₅₀ = 26 μ M). Upon exposure to low light dose (≈ 1.5 J/cm²) aza-BODIPYs **1a** and **2a** showed increased cytotoxicity while all other aza-BODIPYs showed similar cytotoxicity, suggesting that not all aza-BODIPY-mediated cytotoxicity is increased by light irradiation. Furthermore, the 2,6-dibrominated aza-BODIPYs 1b-3b showed significantly higher comparative singlet oxygen quantum yields than the corresponding 2,6-unsubstituted aza-BODIPYs 1a-3a, determined using DPBF as acceptor. Interestingly, the dibrominated aza-BODIPY-diGln 4b shows a marked decreased ability for singlet oxygen production compared with all other aza-BODIPYglutamine conjugates. The comparative singlet oxygen quantum yields did not correlate with the phototoxicity in cells because the intracellular site(s) of singlet oxygen generation, and other cytotoxic species, determine the mechanisms and efficacy of cell death.[12] These results suggest that the cytotoxicity and the ability of the aza-BODIPYs for producing singlet oxygen, depends not only on the presence of bromine atoms at the 2,6-positions but also on the number and substitution of the glutamine groups on the boron atom. In particular, the formation of a cyclic N,O-bidentate aza-BODIPY-Gln, as in 3a,b, induces the highest cytotoxicity, while substitution of the boron atom with two glutamine groups and the presence of 2,6-bromines leads to a significant decrease in singlet oxygen production.

The concentration-dependent cellular uptake of aza-BODIPYs 1a-4a was investigated over a 24 h time period and the results are shown in Figure S22 of the Supplementary Materials. All aza-BODIPYs internalized quickly in the first 2 h, after which a plateau was reached. The BF₂-aza-BODIPY **1a** was found to

974





accumulate the most within cells at all time points investigated, probably due to its higher hydrophobicity compared with the glutamine-substituted aza-BODIPYs. The aza-BODIPY-Gln conjugates showed similar uptake into the HEp2 cells.

Conclusions

A series of novel linker-free near-IR aza-BODIPY-glutamine conjugates were prepared by direct functionalization of the boron atom using Boc-protected L-glutamine. The glutamine group attaches to the aza-BODIPY once or twice through the carboxylate group, producing mono- and di-functionalized aza-BODIPYs, respectively, or via both the carboxylate and the Boc-protected amine to form a cyclic N,O-bidentate five-membered ring. Bromination of the 2,6-positions of the aza-BODIPYs using Nbromosuccinimide gave the corresponding dibrominated derivatives in quantitative yields. The structural features of all aza-BODIPYs were confirmed by ¹H, ¹³C and ¹¹B NMR, HRMS, DFT calculations, and in the case of 3a, via X-ray crystallography. Photophysical measurements showed that the mode and number of glutamine conjugation on the boron atom affects the absorption and emission wavelengths of the aza-BODIPYs; while the cyclic N,O-bidentate BODIPYs display hypsochromic-shifted absorbance bands, the di-Gln displayed bathochromic-shifted emissions. The 2,6-dibrominated BODIPYs showed quenching of the fluorescence and enhanced singlet oxygen quantum yields due to the heavy atom effect. The aza-BODIPYs with cyclic N,Obidentate glutamine on boron displayed the highest cytotoxicity among all aza-BODIPY conjugates in in vitro cell studies, making them promising bifunctional anticancer agents.

Experimental Section

General Data: All commercially available chemical reagents and solvents were purchased from Sigma-Aldrich or VWR and used without further purification. All product yields refer to isolated yields after column chromatography using Sorbent Technologies silica gel (60 Å, 230– 400 mesh). Reactions were monitored using polyester backed 0.2 mm Micro SiliaPlate™ thin-layer chromatography (TLC) plates (SiliCycle Inc.). All ¹H, ¹³C, and ¹¹B NMR spectra were collected using a Bruker AV-400 or AV-500 spectrometer at 300 K in deuterated chloroform (CDCl₃). Chemical shifts (δ) are reported in ppm where CDCl₃ (7.26 ppm for ¹H and 77.0 ppm for ¹³C) is used as references by operating at 400 MHz for ¹H NMR and 126 MHz for ¹³C NMR. BF₃•OEt₂ was used as the reference (0.00 ppm) for ¹¹B NMR spectra. High-resolution mass spectra were collected using an Agilent 6230-B ESI-TOF mass spectrometer in positive mode. UV/ Vis absorption spectra of ca. 10^{-5} M solutions of aza-BODIPYs were recorded. Emission spectra ($\lambda_{\rm ex} = 630$ nm) of ca. 10^{-5} M solutions were recorded in quartz cells. Relative fluorescence quantum yields $(\Phi_{\rm f})$ were calculated using aza-BODIPY **1a** $(\Phi_{\rm f}=0.23$ in chloroform)[10] as the standard using the following equation:

$$\Phi_x = \Phi_{ST} \frac{Grad_x}{Grad_{ST}} \Big(\frac{\eta_x}{\eta_{ST}}\Big)^2$$

where Φ_x and Φ_{ST} are the quantum yields of the sample and standard, Grad_x and Grad_{ST} are the gradient from the plot of integrated fluorescence intensity vs. absorbance, and η is the refractive index

of the solvent. Aza-BODIPYs ${\bf 1a}$ and ${\bf 1b}$ were prepared as previously reported in the literature. [10]

X-ray Crystal Structure Determination: The crystal structure of a hexane/water solvate of **3a** was determined at T = 90K from data collected to θ_{max} = 55.7° on a Bruker Kappa Apex-II diffractometer equipped with a Cu- K_{α} microfocus source. 31,592 measured reflections yielded 14,027 unique data ($R_{int} = 0.056$), of which 10,895 had $I > 2\sigma(I)$. C₄₄H₄₂BN₅O₇. 1/2 C₆H₁₄•0.25H₂O, triclinic space group *P*1, a = 12.5540(5), b = 12.6120(5), c = 30.0243(13) Å, α = 78.971(2), β = 84.982(3), $\gamma = 77.465(2)^{\circ}$, $V = 4549.5(3) \text{ Å}^3$, Z = 4. Absorption corrections were by the multi-scan method. Non-hydrogen atoms were treated with anisotropic displacement parameters. The H atoms were placed in idealized positions, but the water H positions were not located. The asymmetric unit contains four aza-BODIPY molecules, two hexane molecules, one water molecule, and some disordered solvent which was removed using the SQUEEZE procedure. Refinement yielded R = 0.091 for the $I > 2\sigma(I)$ data, $wR(F^2) = 0.241$ for all data and 2170 parameters. $\Delta \rho$ max = 0.50e Å⁻³, $\Delta \rho$ min = -0.31e Å⁻³. The CIF has been deposited at the Cambridge Crystallographic Data Centre, CCDC 1962380.

CCDC 1962380 (for **3a**) contains the supplementary crystallographic data for this paper. These data can be obtained free of charge from The Cambridge Crystallographic Data Centre.

Cellular Studies: All cell culture media and reagents were purchased from Invitrogen unless otherwise stated. Human epithelial type 2 (HEp2) cells (ATCC CCL-23) were purchased from ATCC and maintained at 37 °C under 5 % CO₂ in Eagle's Minimum Essential Medium (MEM) augmented with 10 % fetal bovine serum (FBS) and 1 % penicillin-streptomycin (P/S). Working stock solutions of aza-BODIPYs were prepared at 32 mM in 4 % DMSO and 1 % Cremophor-EL.

Dark Toxicity: HEp2 cells were plated in a Corning Costar 96-well plate and allowed to grow for 24–48 h to reach approximately 10,000 cells per well. Working stock solutions of aza-BODIPYs were diluted with augmented MEM to 400 μм. Cells were exposed to aza-BODIPYs at concentrations of 6.25, 12.5, 25, 50, 100 and 200 μм and then incubated overnight (20–24 h) at 37 °C under 5 % CO₂. Immediately following incubation, the loading medium was removed, and cells were washed with 1X phosphate buffered saline (PBS) in triplicate to remove residual aza-BODIPY. Cells were fed augmented MEM with 20 % CellTiter Blue (CTB) reagent (Promega, Madison WI) and incubated for 4 h at 37 °C under 5 % CO₂. Cell viability was determined by fluorescence intensity at ex. 570/em. 615 nm using a FLUOstar OPTIMA microplate reader (BMG Labtech, Cary NC). Cell dark toxicity is expressed as a percentage of viable cells.

Phototoxicity: HEp2 cells were plated in a Corning Costar 96-well plate and allowed to grow 24–48 h to reach approximately 10,000 cells per well. Working stock solutions of aza-BODIPYs were diluted with augmented MEM to 200 μm. Cells were exposed to aza-BODIPYs at concentrations of 3.125, 6.25, 12.5, 25, 50 and 100 μm and then incubated overnight (20–24 h) at 37 °C under 5 % CO₂. Immediately following incubation, the loading medium was removed, and cells were washed 1X PBS. Cells were fed augmented MEM and exposed to a light dose of \approx 1.5 J/cm² generated using a 600 W Quartz Tungsten Halogen lamp (Newport Corporation, Irvine CA). Cells were exposed for 20 min while the 96-well plate rested on an EchoTherm IC₅₀ chilling/heating plate (Torrey Pines Scientific, Carlsbad CA) set to 5 °C to maintain ambient temperature. Following light exposure, loading media was removed and cells were fed augmented MEM with 20 % CTB reagent (Promega, Madison WI)





and incubated for 4 h at 37 °C under 5 % CO₂. Cell viability was determined by fluorescence intensity at ex. 570/em. 615 nm using a FLUOstar OPTIMA microplate reader. Cell phototoxicity is expressed as a percentage of viable cells.

Time-Dependent Cellular Uptake: HEp2 cells were plated in a Corning Costar 96-well plate and allowed to grow for 24-48 h to reach approximately 10,000 cells per well. Working stock solutions of aza-BODIPYs were diluted with augmented MEM to 20 μm. Cells were exposed to aza-BODIPYs at a final concentration of 10 μm at 0, 1, 2, 4, 8 and 24 h time intervals. Following treatment, the loading media was removed, and cells were washed with 1X PBS in triplicate, and then solubilized with 0.25 % Triton X-100 (Calbiochem, San Diego, CA) in 1X PBS. An aza-BODIPY standard curve (10, 5, 2.5, 1.25, 0.625 and 0.3125 µm) and a cell standard curve (10,000, 20,000, 40,000, 60,000, 80,000 and 100,000 cells per well) were also generated. The CyQUANT Cell Proliferation Assay Kit (Invitrogen, Carlsbad CA) was utilized for cell quantification. Aza-BODIPY concentrations were determined by fluorescence intensity at ex. 640/em. 680 nm using a FLUOstar OPTIMA microplate reader. The cellular uptake is expressed in nm of aza-BODIPY per cell.

Comparative Singlet Oxygen Quantum Yield: To each well of a 6-well plate was added 2 mL containing 50 μ m of 1,3-diphenylisobenzofuran (DPBF) and 5 μ m of each photosensitizer in DMSO with 1 % Cremophor-EL. The plate was irradiated using a 71 W filtered light source of > 500 nm with a Schott glass 500 nm long-pass yellow filter for 1 h. At 15 min increments, 200 μ L aliquots were removed from each of the six wells and the absorbance was measured at 410 nm. The rate of singlet oxygen generation was determined by the decrease in intensity of absorbance of DPBF over time. Irradiation of DPBF-DMSO solution in the absence of photosensitizer as a negative control, and solution of DPBF/methylene blue/DMSO as a reference standard were also performed. Singlet oxygen quantum yields were determined using the equation:

$$\Phi_{\Delta(x)} = \Phi_{\Delta(std)} \times \frac{S_x}{S_{std}}$$

where $\Phi_{\Delta(x)}$ is the singlet oxygen quantum yield of the sample, $\Phi_{\Delta(\text{std})}$ is the singlet oxygen quantum yield of the standard (methylene blue, 0.52), S_x is the slope of the plot of absorbance vs. time of the sample, and S_{std} is the slope of the plot of absorbance vs. time of the standard. [11]

Computational Modeling: The geometries of all BODIPYs were optimized at the B3LYP/6-31G(d,p) level^[13] without symmetry constraints. For **1a–3a** and **1b–3b**, the stationary points on the potential energy surface were confirmed with frequency calculations. The solvent effects were taken into account using the Polarized Continuum Model (PCM).^[14] The UV/Vis absorption data were calculated using the TD-DFT method^[15] at the M06-2X/6-31+G(d,p) level^[16] as recommended in the literature.^[17]All calculations were performed using the Gaussian 09 program package.^[18]

General Synthesis of Aza-BODIPY 2a–4a: Aza-BODIPY **1a** (50.0 mg, 0.090 mmol) was dissolved in 10 mL of dry dichloromethane under a nitrogen atmosphere, followed by the addition of BCl₃ (1 M in toluene, 0.18 mL, 0.180 mmol). The reaction mixture was stirred for 1 h at room temperature. Then the $N\alpha$ -(tert-butoxy-carbonyl)-L-glutamine (110.5 mg, 0.450 mmol) in 2 mL of dry dichloromethane and 10 drops of dry triethylamine was added dropwise. The final mixture was stirred at room temperature for 2 h. The reaction mixture was then quenched with saturated aqueous NaHCO₃, extracted with dichloromethane, and then washed with saturated brine. The organic layers were combined and dried over

anhydrous Na_2SO_4 . The organic solvent was removed under reduced pressure and the residue was purified by preparative TLC using DCM/MeOH: $NH_4OH = 95$: 4: 1 for elution, yielding 25.7 % mono-substituted aza-BODIPY **2a** (18.0 mg, 0.023 mmol), 10.5 % cyclicaza-BODIPY**3a** (7.2 mg, 0.009 mmol) and 7.8 % di-substituted aza-BODIPY **4a** (7.0 mg, 0.007 mmol).

Aza-BODIPY 2a: M.p. 98–102 °C; ¹H NMR (400 MHz, CDCl₃) δ = 8.07 (d, J = 8.9 Hz, 4H), 7.94–7.89 (m, 4H), 7.53–7.41 (m, 6H), 6.99 (d, J = 8.8 Hz, 4H), 6.86 (d, J = 6.5 Hz, 2H), 6.41 (bs, 1H), 5.18 (bs, 1H), 4.72 (d, J = 7.0 Hz, 1H), 3.90 (s, 6H), 3.18 (dd, J = 13.1, 7.7 Hz, 1H), 1.88–1.71 (m, 2H), 1.34 (s, 9H), 1.11–1.00 (m, 1H), 0.98–0.91 (m, 1H); ¹³C NMR (126 MHz, CDCl₃) δ = 174.56, 171.04, 161.08, 158.56, 158.37, 155.58, 145.49, 145.40, 144.11, 143.96, 131.59, 131.09, 131.07, 130.86, 130.74, 129.51, 129.46, 129.41, 129.36, 128.64, 128.53, 125.31, 117.52, 117.28, 114.21, 79.58, 55.45, 52.76, 32.14, 31.60, 28.74, 28.24, 22.67, 14.13; ¹¹B NMR (128 MHz, CDCl₃) δ = 0.37 (d, J = 25.5 Hz); HRMS (ESI-TOF): m/z [M + Na]⁺, 806.31370 calcd. for C₄₄H₄₃BFN₅NaO₇, 806.31393.

Aza-BODIPY 3a: M.p. 97–98 °C; ¹H NMR (400 MHz, CDCl₃) δ = 8.07 (t, J = 8.6 Hz, 4H), 7.51 (dd, J = 6.6, 3.0 Hz, 2H), 7.45–7.39 (m, 6H), 7.33 (bs, 2H), 7.02 (dd, J = 9.0, 3.1 Hz, 4H), 6.86 (bs, 1H), 6.68 (s, 1H), 6.67 (s, 1H), 5.16 (bs, 1H), 3.92 (s, 6H), 2.04–1.89 (m, 2H), 1.83 (dd, J = 9.7, 3.4 Hz, 1H), 1.14 (s, 9H), 1.07–0.92 (m, 1H), –0.48 (dd, J = 14.7, 9.6 Hz, 1H); ¹³C NMR (126 MHz, CDCl₃) δ = 175.63, 175.02, 162.32, 161.37, 161.29, 160.27, 155.35, 146.05, 145.21, 144.80, 143.91, 132.39, 131.92, 131.11, 130.98, 130.37, 129.88, 129.00, 128.86, 128.32, 125.21, 125.07, 119.13, 117.76, 114.46, 114.42, 79.02, 56.72, 55.50, 53.43, 32.35, 28.19, 23.68; ¹¹B NMR (128 MHz, CDCl₃) δ = 1.63 (s); HRMS (ESI-TOF): m/z [M + H]⁺, 764.32598 calcd. for $C_{44}H_{43}BN_5O_7$, 764.32576.

Aza-BODIPY 4a: M.p. 118–119 °C; ¹H NMR (400 MHz, CDCl₃) δ = 8.13–8.07 (m, 4H), 7.80–7.71 (m, 4H), 7.53–7.45 (m, 6H), 6.99 (d, J = 8.9 Hz, 4H), 6.84 (s, 2H), 6.71 (bs, 1H), 5.38–5.26 (m, 2H), 5.14–5.01 (m, 2H), 3.91 (s, 6H), 3.78–3.69 (m, 2H), 2.16–1.99 (m, 4H), 1.52–1.42 (m, 4H), 1.36 (s, 18H); ¹³C NMR (126 MHz, CDCl₃) δ = 171.39, 161.17, 157.94, 155.78, 146.07, 144.18, 131.56, 131.26, 130.94, 129.15, 128.76, 125.23, 117.77, 114.16, 79.89, 70.61, 55.46, 53.39, 31.94, 28.89, 28.26, 22.70, 14.13; ¹¹B NMR (128 MHz, CDCl₃) δ = 0.07 (s); HRMS (ESI-TOF): m/z [M + Na]⁺, 1032.43081 calcd. for C₅₄H₆₀BN₇NaO₁₂, 1032.42943.

General Synthesis of Aza-BODIPY 2b–4b: Aza-BODIPYs **2a–4a** (0.009 mmol) was dissolved in 2 mL of chloroform, followed by the addition of *N*-bromosuccinimide (0.020 mmol). The reaction mixture was stirred at room temperature until TLC shows the disappearance of staring material. The reaction mixture was then quenched with saturated aqueous NaHCO₃, extracted with dichloromethane, and then washed with water and saturated brine. The organic layers were combined and dried over anhydrous Na₂SO₄. The organic solvent was removed under reduced pressure. Aza-BODIIPYs **2b–4b** were isolated in quantitative yields.

Aza-BODIPY 2b: M.p. 136–138 °C; ¹H NMR (400 MHz, CDCl₃) $\delta = 7.96-7.89$ (m, 4H), 7.68-7.63 (m, 2H), 7.61-7.56 (m, 2H), 7.51-7.43 (m, 6H), 6.98 (dd, J = 1.8 Hz, 4H), 6.46 (bs, 1H), 5.21 (bs, 1H), 4.67 (d, 1H), 3.89 (s, 6H), 3.01 (m, 1H), 1.81–1.73 (m, 2H), 1.45 (bs, 1H), 1.43 (bs, 1H), 1.40 (s, 9H); 13 C NMR (126 MHz, CDCl₃) $\delta = 177.02$, 174.61, 173.00, 171.20, 161.10, 132.61, 132.57, 130.97, 130.71, 130.36, 129.97, 129.62, 129.36, 128.25, 128.16, 123.42, 113.68, 79.74, 55.40, 31.58, 28.69, 28.29, 28.27, 28.22, 22.64, 22.55, 14.09; 11 B NMR (128 MHz, CDCl₃) $\delta = -0.35$ (d, J = 24.3 Hz); HRMS (ESI-TOF): m/z [M + Na]⁺, 964.12864; calcd. for C₄₄H₄₁BBr₂FN₅NaO₇, 964.13338.

Aza-BODIPY 3b: M.p. 110–113 °C; ¹H NMR (400 MHz, CDCl₃) δ = 7.95 (dd, J = 20.0, 8.8 Hz, 4H), 7.52–7.42 (m, 8H), 7.32–7.27 (m, 1H),

976





7.15–7.08 (m, 1H), 7.01 (d, J=8.3 Hz, 4H), 6.77 (bs, 1H), 5.27 (bs, 1H), 3.91 (s, 6H), 1.97–1.90 (m, 2H), 1.18 (s, 9H), 1.01 (bs, 2H), -0.55 to -0.69 (m, 1H); 13 C NMR (126 MHz, CDCl₃) $\delta=174.79$, 161.32, 160.19, 159.03, 154.88, 144.58, 142.91, 141.82, 132.44, 132.30, 130.43, 129.90, 129.17, 128.87, 128.68, 123.20, 113.92, 113.82, 79.35, 56.66, 55.44, 32.36, 29.69, 28.29, 23.46; 11 B NMR (128 MHz, CDCl₃) $\delta=1.46$ (s); HRMS (ESI-TOF): m/z [M + H]⁺ 922.14707; calcd. for $C_{44}H_{41}BBr_2N_5O_7$, 922.14521.

Aza-BODIPY 4b: M.p. 137–141 °C; ¹H NMR (500 MHz, CDCl₃) $\delta = 7.97$ (d, J = 8.7 Hz, 4H), 7.52–7.46 (m, 5H), 7.44–7.36 (m, 5H), 6.97 (d, J = 8.8 Hz, 4H), 6.74 (s, 2H), 5.34 (s, 2H), 5.10 (d, J = 6.3 Hz, 2H), 3.89 (s, 6H), 3.70 (d, J = 6.9 Hz, 2H), 2.09 (s, 4H), 1.41 (s, 18H); 13 C NMR (126 MHz, CDCl₃) $\delta = 161.19$, 144.91, 132.78, 132.26, 130.86, 130.19, 129.65, 128.43, 123.42, 113.60, 99.97, 80.02, 55.41, 32.45, 29.69, 29.02, 22.68, 14.08; 11 B NMR (128 MHz, CDCl₃) $\delta = -0.76$ (s); HRMS (ESI-TOF): m/z [M + Na]⁺, 1190.24503 calcd. for C₅₄H₅₈BBr₂N₇O₁₂Na, 1190.24910.

Conflicts of Interest: The authors declare no conflict of interest.

Acknowledgments

This work was supported by the National Science Foundation, grant number CHE-1800126. The authors thank the Louisiana Optical Network Initiative (www.loni.org) for the use of their computer facilities.

Keywords: Photodynamic therapy · Photosensitizer · Aza-BODIPYs · N-Boc-L-glutamine

- a) T. J. Dougherty, C. J. Gomer, B. W. Henderson, G. Jori, D. Kessel, M. Korbelik, J. Moan, Q. Peng, J. Natl. Cancer Inst. 1998, 90, 889–905; b) R. Pandey, G. Zheng, In the Porphyrin Handbook, Vol. 6 (Eds.: K. M. Kadish; K. M. Smith; R. Guilard), Boston, Massachusetts, 2000, pp. 157–230; c) H. Abrahamse, M. R. Hamblin, Biochem. J. 2016, 473, 347–364.
- [2] a) M. A. T. Rogers, J. Chem. Soc. 1943, 590–596; b) M. Rogers, Nature 1943, 151, 504; c) W. H. Davies, M. A. T. Rogers, J. Chem. Soc. 1944, 126– 131
- [3] a) Y. Ge, D. F. O'Shea, Chem. Soc. Rev. 2016, 45, 3846–3864; b) E. Bodio,
 F. Denat, C. Goze, J. Porphyrins Phthalocyanines 2019, 23, 1159–1183.
- [4] a) S. G. Awuah, Y. You, RSC Adv. 2012, 2, 11169–11183; b) A. Kamkaew, S. H. Lim, H. B. Lee, L. V. Kiew, L. Y. Chung, K. Burgess, Chem. Soc. Rev. 2013, 42, 77–88; c) G. Fan, L. Yang, Z. Chen, Front. Chem. Sci. Eng. 2014, 8, 405–417; d) A. Turksoy, D. Yildiz, E. U. Akkaya, Coord. Chem. Rev. 2019, 379, 47–64.

- [5] a) M. Zhao, Y. Xu, M. Xie, L. Zou, Z. Wang, S. Liu, Q. Zhao, Adv. Healthcare Mater. 2018, 7, e1800606; b) L. Jiao, W. Pang, J. Zhou, Y. Wei, X. Mu, G. Bai, E. Hao, J. Org. Chem. 2011, 76, 9988–9996.
- [6] a) J. Murtagh, D. O. Frimannsson, D. F. O'Shea, Org. Lett. 2009, 11, 5386–5389; b) A. Palma, L. A. Alvarez, D. Scholz, D. O. Frimannsson, M. Grossi, S. J. Quinn, D. F. O'Shea, J. Am. Chem. Soc. 2011, 133, 19618–19621; c) S. Bhuniya, M. H. Lee, H. M. Jeon, J. H. Han, J. H. Lee, N. Park, S. Maiti, C. Kang, J. S. Kim, Chem. Commun. 2013, 49, 7141–7143; d) D. Wu, D. F. O'Shea, Org. Lett. 2013, 15, 3392–3395; e) W.-J. Shi, R. Menting, E. A. Ermilov, P.-C. Lo, B. Röder, D. K. Ng, Chem. Commun. 2013, 49, 5277–5279; f) D. Collado, Y. Vida, F. Najera, E. Perez-Inestrosa, RSC Adv. 2014, 4, 2306–2309; g) D. Wu, S. Cheung, M. Devocelle, L.-J. Zhang, Z.-L. Chen, D. F. O'Shea, Chem. Commun. 2015, 51, 16667–16670.
- [7] a) A. L. Nguyen, M. Wang, P. Bobadova-Parvanova, Q. Do, Z. Zhou, F. R. Fronczek, K. M. Smith, M. G. H. Vicente, J. Porphyrins Phthalocyanines 2016, 20, 1409–1419; b) G. Zhang, M. Wang, F. R. Fronczek, K. M. Smith, M. G. H. Vicente, Inorg. Chem. 2018, 57, 14493–14496; c) M. Wang, M. G. H. Vicente, D. Mason, P. Bobadova-Parvanova, ACS Omega 2018, 3, 5502–5510; d) M. Wang, G. Zhang, P. Bobadova-Parvanova, A. N. Merriweather, L. Odom, D. Barbosa, F. R. Fronczek, K. M. Smith, M. G. H. Vicente, Inorg. Chem. 2019, 58, 11614–11621; e) E. Bodio, C. Goze, Dyes Pigm. 2019, 160, 700–710; f) Z. Wang, C. Cheng, Z. Kang, W. Miao, Q. Liu, H. Wang, E. Hao, J. Org. Chem. 2019, 84, 2732–2740.
- [8] J. Pliquett, A. Dubois, C. Racoeur, N. Mabrouk, S. Amor, R. Lescure, A. Bettaïeb, B. Collin, C. Bernhard, F. Denat, *Bioconjugate Chem.* 2019, 30, 1061–1066.
- [9] a) A. L. Miller, Altern. Methods Toxicol. 1999, 4, 239–248; b) M. A. Medina, J. Nutr. 2001, 131, 25395–2542S.
- [10] a) A. Gorman, J. Killoran, C. O'Shea, T. Kenna, W. M. Gallagher, D. F. O'Shea, J. Am. Chem. Soc. 2004, 126, 10619–10631; b) S. Kumar, T. K. Khan, M. Ravikanth, Tetrahedron 2015, 71, 7608–7613.
- [11] S. H. Lim, C. Thivierge, P. Nowak-Sliwinska, J. Han, H. Van Den Bergh, G. Wagnieres, K. Burgess, H. B. Lee, J. Med. Chem. 2010, 53, 2865–2874.
- [12] J. H. Gibbs, Z. Zhou, D. Kessel, F. R. Fronczek, S. Pakhomova, M. G. H. Vicente, J. Photochem. Photobiol. B 2015, 145, 35–47.
- [13] a) R. J. Sension, S. T. Repinec, A. Z. Szarka, R. M. Hochstrasser, J. Chem. Phys. 1993, 98, 6291–6315; b) C. Lee, W. Yang, R. G. Parr, Phys. Rev. B 1988, 37, 785–789.
- [14] J. Tomasi, B. Mennucci, R. Cammi, Chem. Rev. 2005, 105, 2999-3094.
- [15] R. Bauernschmitt, R. Ahlrichs, Chem. Phys. Lett. 1996, 256, 454-464.
- [16] Y. Zhao, D. G. Truhlar, Theor. Chem. Acc. 2008, 120, 215–241.
- [17] B. Le Guennic, D. Jacquemin, Acc. Chem. Res. 2015, 48, 530-537.
- [18] M. Frisch, G. Trucks, H. Schlegel, G. Scuseria, M. Robb, J. Cheeseman, G. Scalmani, V. Barone, B. Mennucci, G. Petersson, *Gaussian Inc., Wallingford, CT* 2009.

Received: December 2, 2019